High Harmonic Generation in Molecules

Chris Greene

Dept. of Physics and JILA

University of Colorado (chris.greene @ colorado.edu)

Support

Dept. of Energy, Basic Energy Sciences, Office of Science

+NSF EUV-ERC

Zach Walters

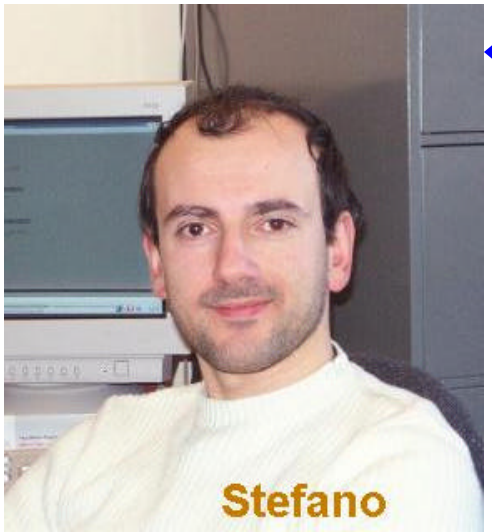

Stefano Tonzani

Collaborators on the *theoretical* projects discussed in this talk

THE UNIVERSITY OF CHICAGO

…bound

Two topics for today's presentation:

1. Preliminary: Towards a quantitative description of high harmonic generation in complex polyatomic molecules following initial excitation by a Raman pulse *(theoretical collaborators – Zachary Walters and Stefano Tonzani; experimental results: N. Wagner, A. Wuest, M. Murnane, H. Kapteyn, et al.)*

– Wagner et al., PNAS 103, 13279 (2006).

2. Caution: Some doubts about attempts thus far to reconstruct molecular orbital spatial shapes using high harmonic generation *(with Stefano Tonzani and Zach Walters)*

Probing Proton Dynamics in Molecules on an Attosecond Time Scale

Talk Topic #1

21 APRIL 2006 VOL 312 SCIENCE 424

S. Baker,[1] J. S. Robinson,[1] C. A. Haworth,[1] H. Teng,[1] R. A. Smith,[1] C. C. Chirilă,[2] M. Lein,[2] J. W. G. Tisch,[1] J. P. Marangos[1]*

We demonstrate a technique that uses high-order harmonic generation in molecules to probe nuclear dynamics and structural rearrangement on a subfemtosecond time scale. The chirped nature of the electron wavepacket produced by laser ionization in a strong field gives rise to a similar chirp in the photons emitted upon electron-ion recombination. Use of this chirp in the emitted light allows information about nuclear dynamics to be gained with 100-attosecond temporal resolution, from excitation by an 8-femtosecond pulse, in a single laser shot. Measurements on molecular hydrogen and deuterium agreed well with calculations of ultrafast nuclear dynamics in the H_2^+ molecule, confirming the validity of the method. We then measured harmonic spectra from CH_4 and CD_4 to demonstrate a few-femtosecond time scale for the onset of proton rearrangement in methane upon ionization.

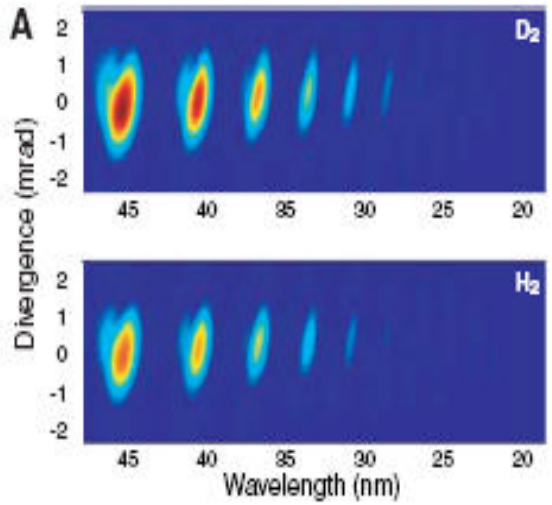

Fig. 3. Harmonic emission in H_2 and D_2. (**A**) Raw CCD images on a common intensity scale (red represents brightest signal, blue weakest) revealing that at all orders observed, harmonic emission is weaker in H_2 than in D_2 at the same density. (**B**)

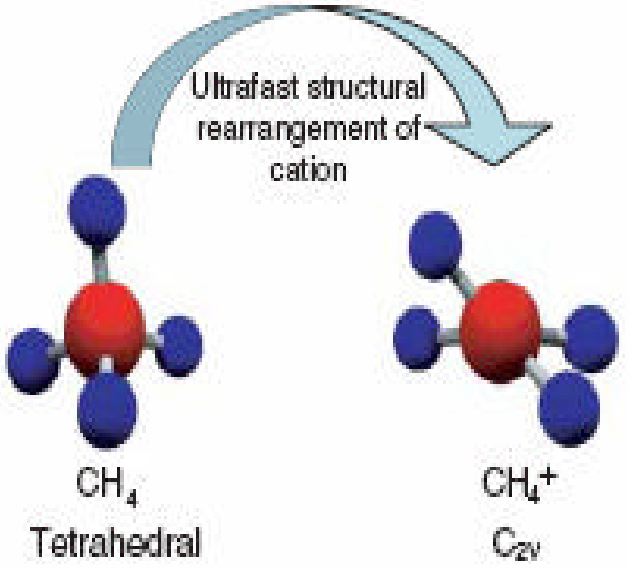

Fig. 4. Probing structural rearrangement in CH_4 and CD_4. (**A**) Ratio of harmonic signals in CD_4 and CH_4 (black). The error represents SE over 200 laser shots. Also shown is the control ratio of two harmonic spectra from CD_4 taken separately (red). (**B**) Known structures of CH_4 and CH_4^+ at equilibrium. Upon removal of an electron, it is anticipated that CH_4 will rapidly evolve toward the CH_4^+ structure shown.

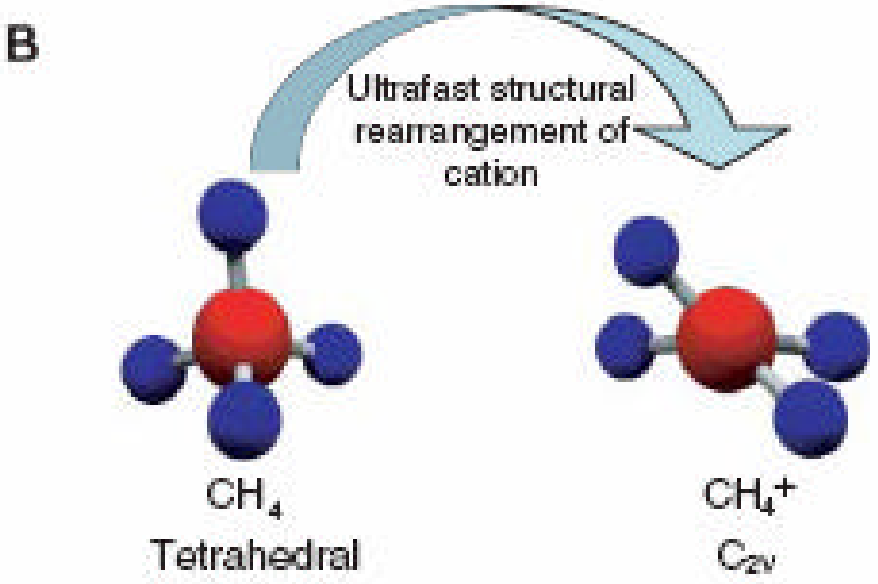

Fig. 4. Probing structural rearrangement in CH_4 and CD_4. (**A**) Ratio of harmonic signals in CD_4 and CH_4 (black). The error represents SE over 200 laser shots. Also shown is the control ratio of two harmonic spectra from CD_4 taken separately (red). (**B**) Known structures of CH_4 and CH_4^+ at equilibrium. Upon removal of an electron, it is anticipated that CH_4 will rapidly evolve toward the CH_4^+ structure shown.

The harmonics are approximately proportional to the squared modulus of the nuclear autocorrelation function, $c(\tau) = \int \chi(R,0)\chi(R,\tau)dR$, where $\chi(R,0)$ and $\chi(R,\tau)$ are the initial and propagated vibrational wavepackets in the molecular ion, R is the internuclear distance, and τ is the electron travel time (equivalent to our delay time, Δt). For

Recently published SF_6 experiment from Wagner, Wuest, Murnane, Kapteyn, et al.

– Use of high harmonic generation to observe quantum beats (a.k.a. – molecular dynamics) between different Raman-excited vibrational modes

– Wagner et al., PNAS 103, 13279 (2006).

Preliminary theoretical analysis presented here: the work of Zach Walters, Stefano Tonzani, and CHG

– Ours is a different picture, not involving the correlation function

$$c(\tau) = \int \chi(R,0)\chi(R,\tau)dR$$

…though this could also be important when hydrogen atoms are moving.

6 vibrational normal modes of SF_6, taken from Wagner et al., 2006 PNAS … *Margaret or Henry could explain the experiment nicely…*

Raman active modes 1,2,5

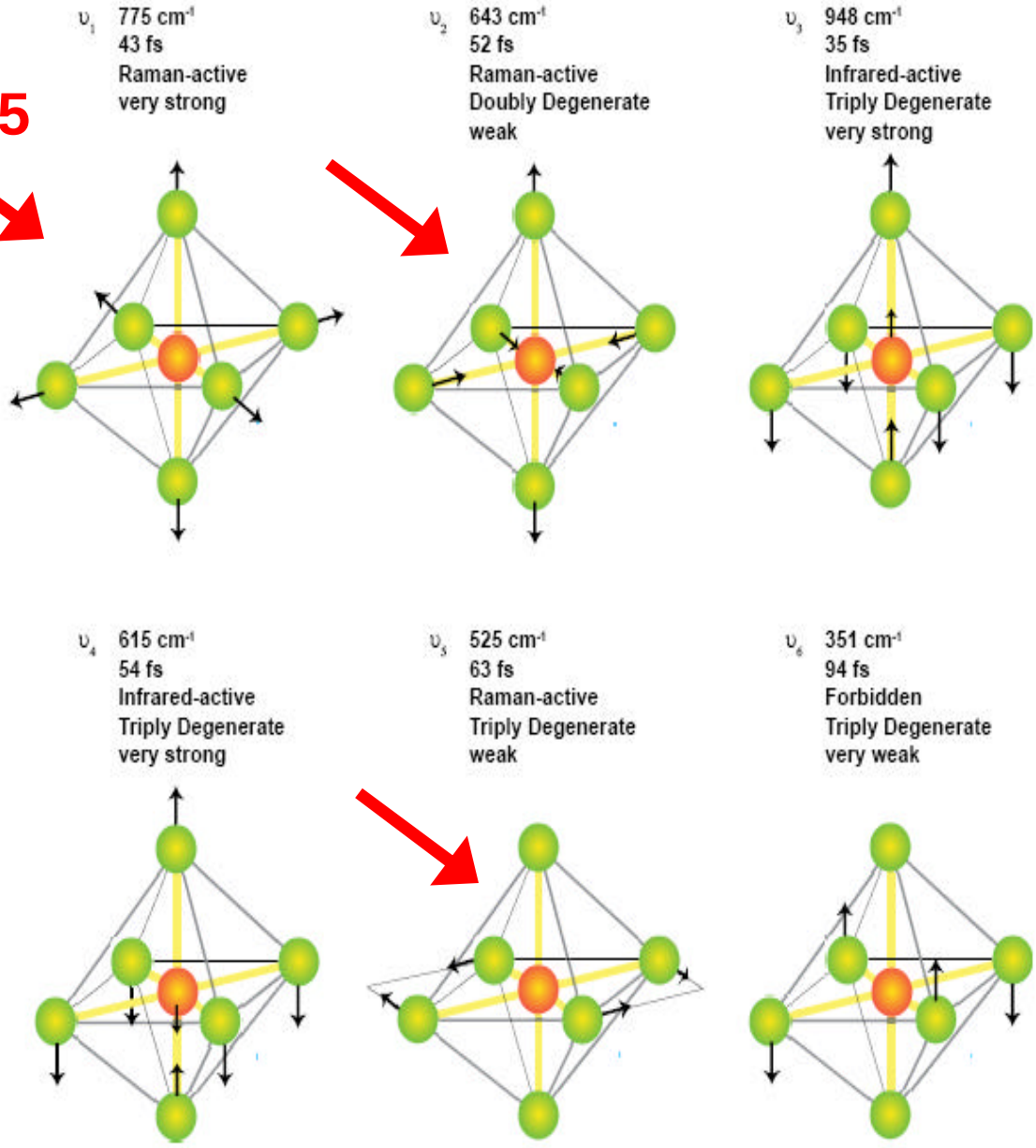

Raman active modes for SF_6

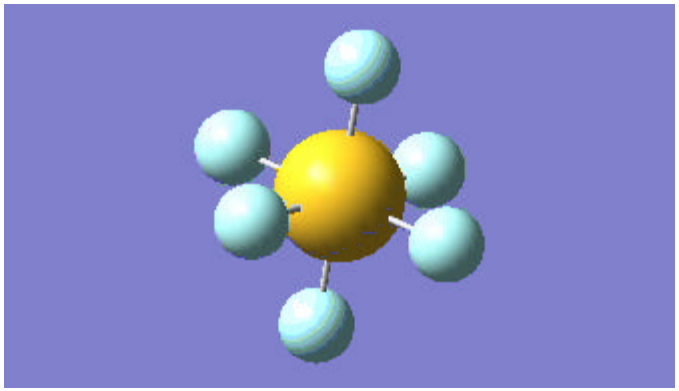

Mode v_1, A_{1g}, symmetric stretch (breathing mode), nondegenerate

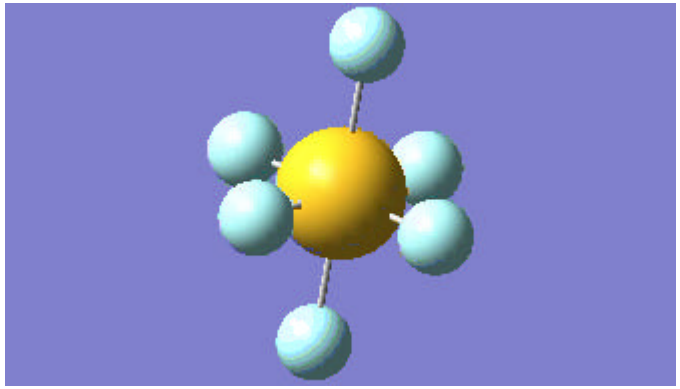

Mode v_2, E_g, doubly degenerate

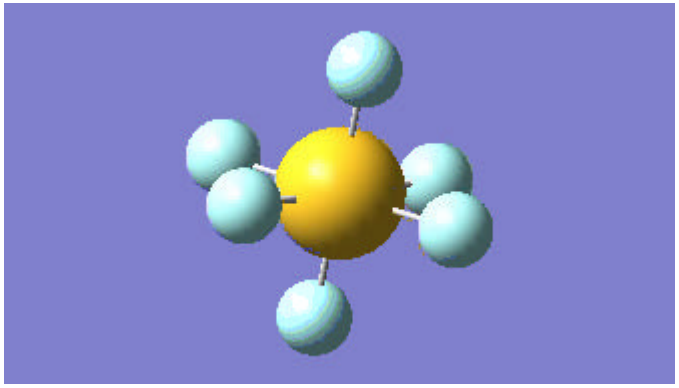

Mode v_5, T_{2g}, triply degenerate

-Excite molecules at t=0 using a perturbative weak Raman pulse, which excites the 3 Raman-active vibrational modes of SF_6.

-Then wait a time T, and hit the molecule with a strong pulse that ionizes and generates a high harmonic photon (39^{th} in this case)

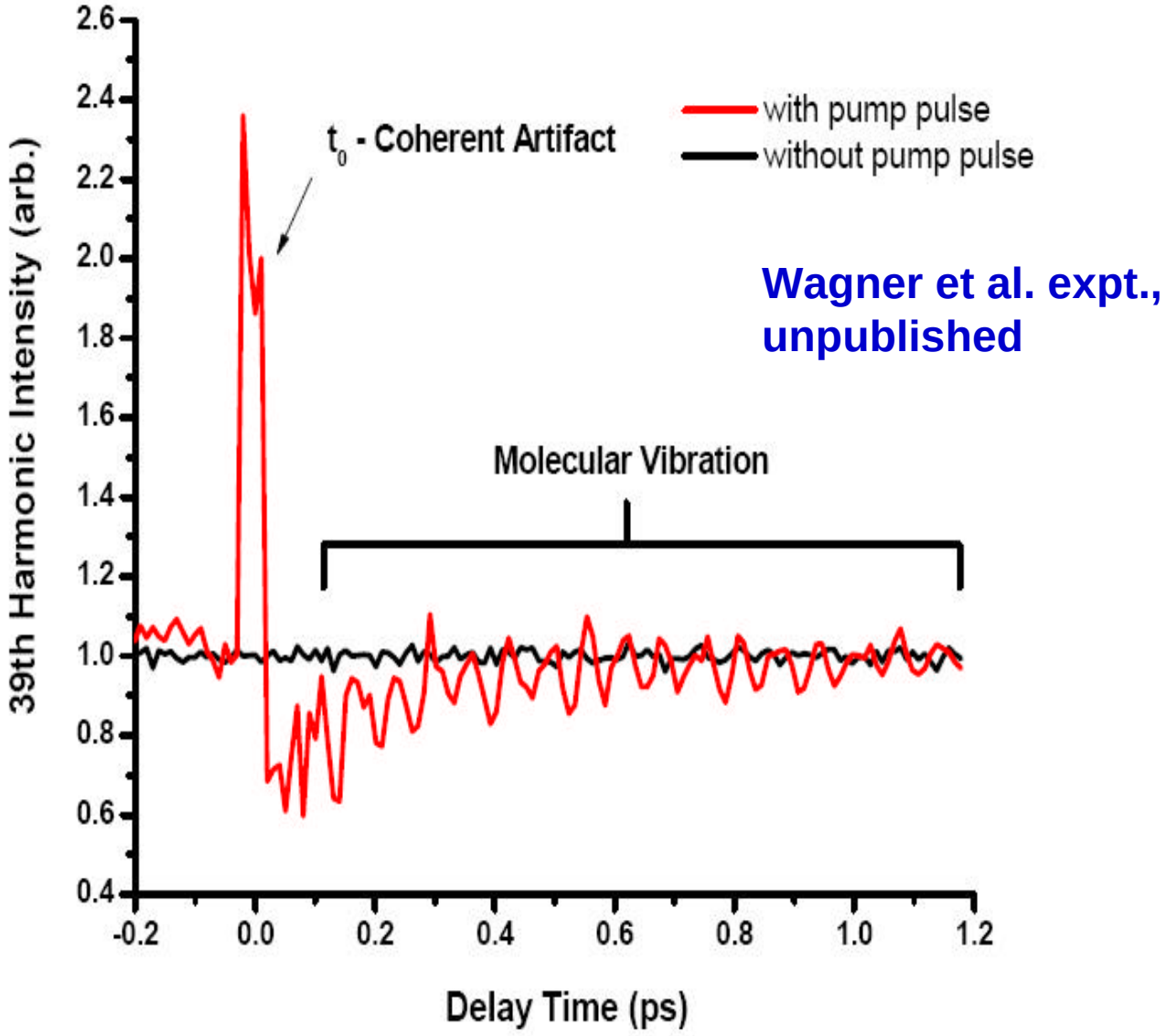

Wagner et al. expt., unpublished

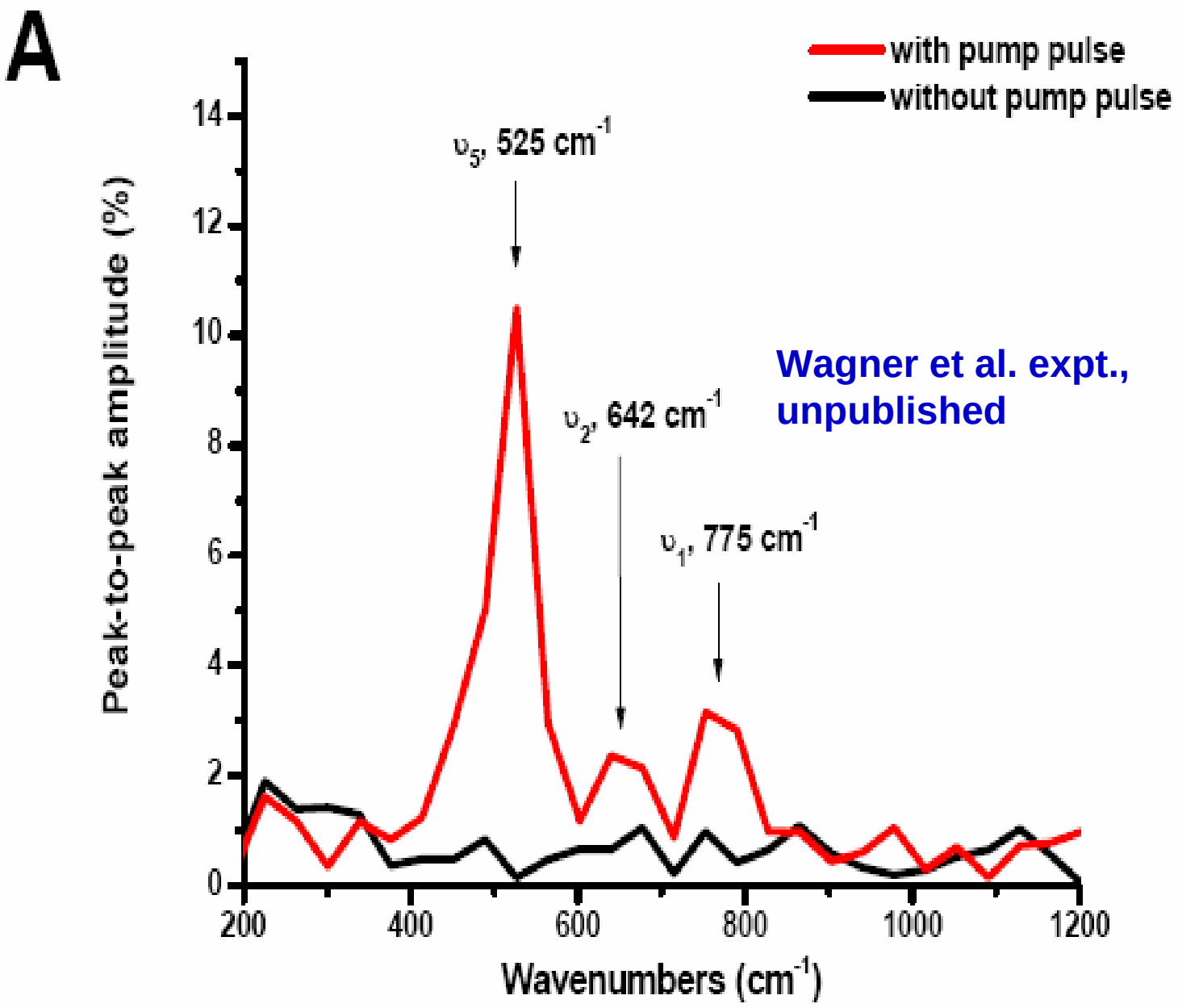
A
with pump pulse
without pump pulse
υ5, 525 cm-1
υ2, 642 cm-1
υ1, 775 cm-1
Wagner et al. expt., unpublished
Peak-to-peak amplitude (%)
Wavenumbers (cm-1)
0
2
4
6
8
10
12
14
200
400
600
800
1000
1200

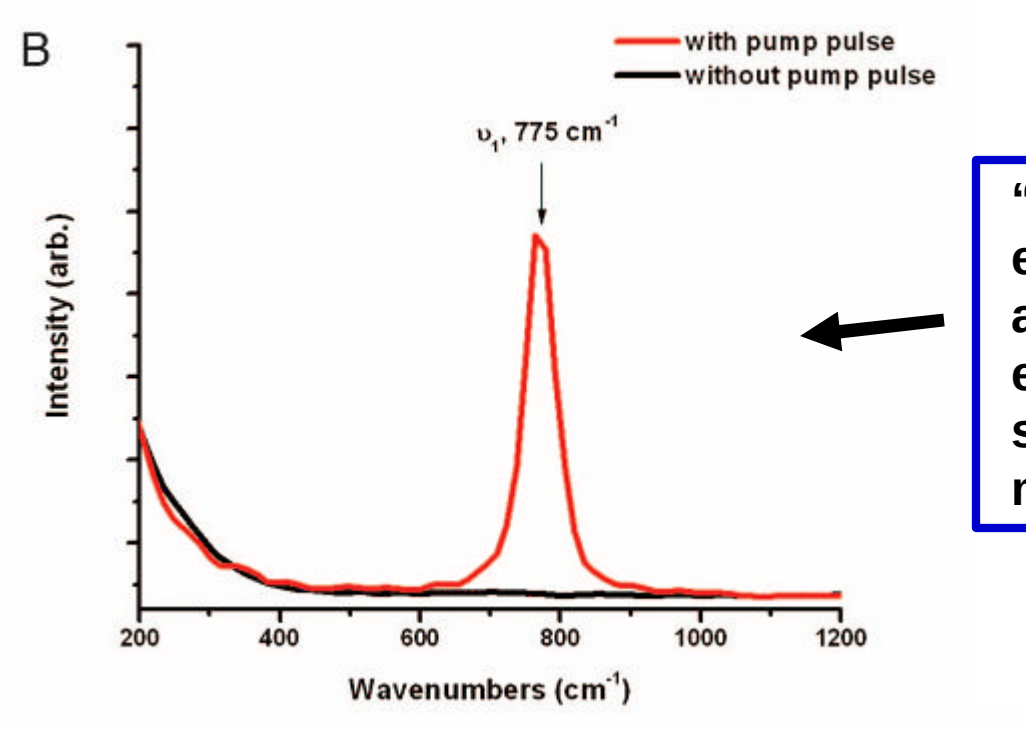

“conventional” Raman experiment shows almost exclusively the excitation of the symmetric stretch mode

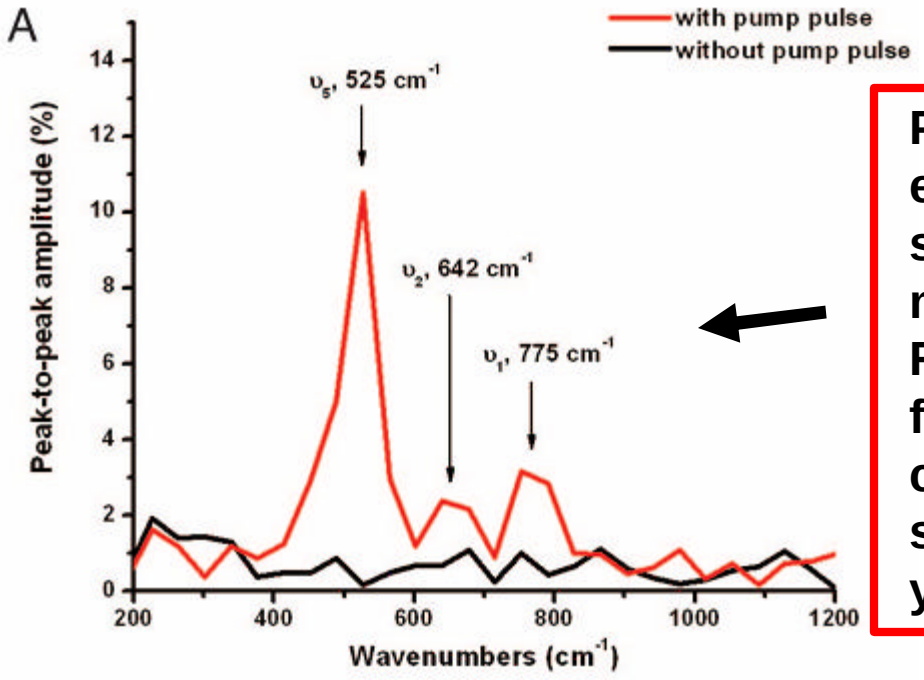

Pump-pulse HHG experiment shows the symmetric stretch mode but two other Raman active modes, far stronger than the conventional Raman spectrum would lead you to expect!

Goals for our theoretical formulation:

1. Understand why the symmetric stretch Raman mode is no longer dominant in this HHG experiment
2. Understand the approximate size of the modulations created in this pump-probe experiment as a function of delay time
3. Improve on simplistic models by using realistic molecular wavefunctions, for both the initial orbital and the rescattering/recombining electron
4. Formulate this as a quantum interference phenomenon, and identify the coherent, indistinguishable pathways involved.

Interpretation of oscillatory structures as *vibrational Raman-excited quantum beats*

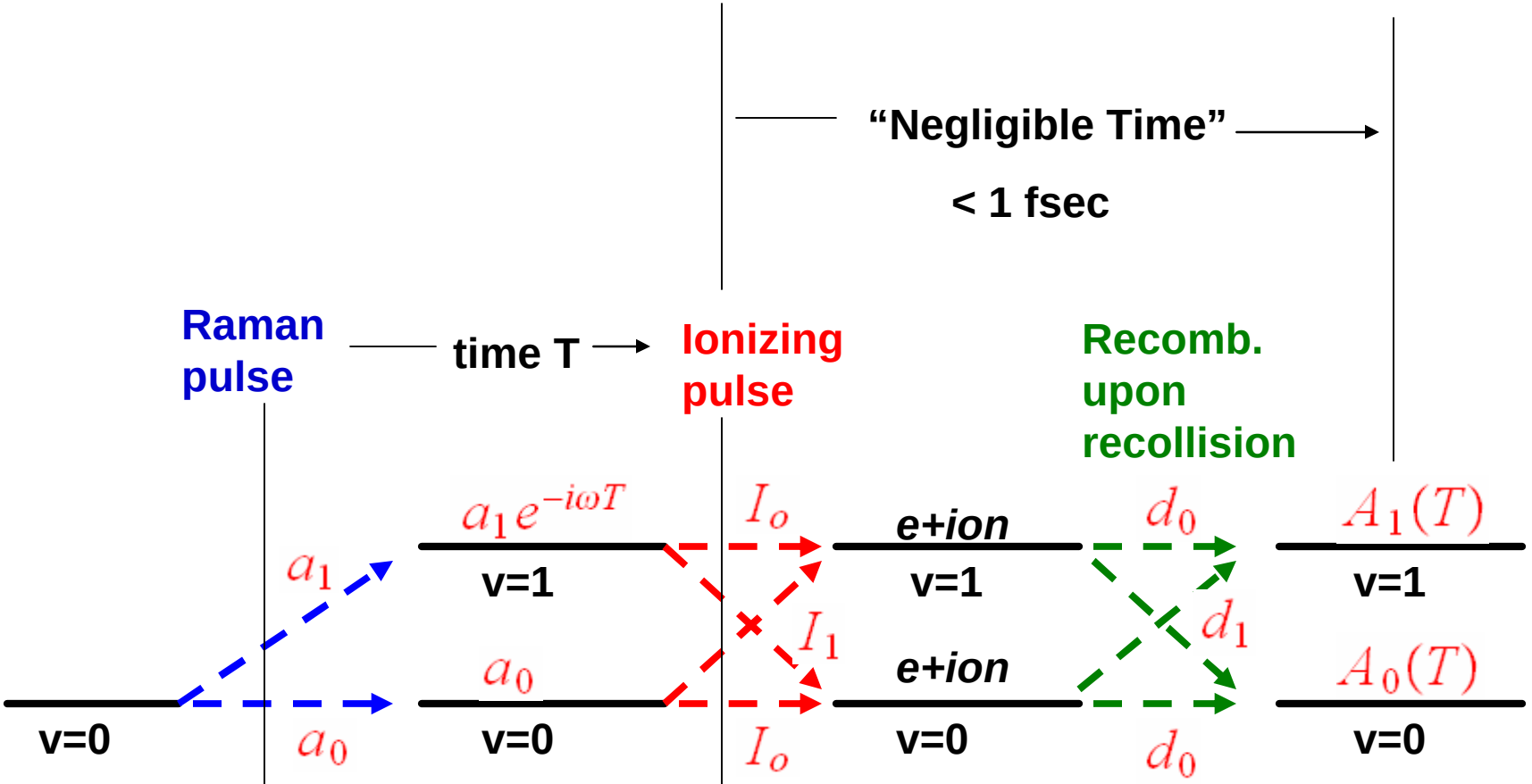

$$Rate(HHG) \propto |A_0(T)|^2 + |A_1(T)|^2$$

Simplest order-of-magnitude estimate: neglect d_1, which gives:

$$A_0(T) \simeq a_0 I_0 + a_1 I_1 e^{-i\omega T}$$

$$A_1(T) \simeq a_0 I_1 + a_1 I_0 e^{-i\omega T}$$

$$Rate(HHG) \propto |A_0(T)|^2 + |A_1(T)|^2$$

And putting this all together, we estimate a final fractional modulation for this one mode, approximately equal to:

$$\text{Modulation Fraction} \simeq 8\left|\frac{a_1}{a_0}\frac{I_1}{I_0}\right| \simeq \begin{array}{|c|}\hline 0.02-0.05, calc \\ \hline 0.02-0.11, \text{exp} \\ \hline \end{array}$$

This picture gives the following for the HHG signal for any given harmonic:

$$d_0^* d_0 + d_1^* d_1 = I_0^* I_0 R_0^* R_0 \left\{ a_0^* a_0 + a_1^* a_1 + 2\mathrm{Re}\left[a_0 a_1^* e^{i\omega\tau} \left(\frac{I_1}{I_0} + \frac{R_1}{R_0} + \frac{I_1^*}{I_0^*} + \frac{R_1^*}{R_0^*} \right) \right] \right\}$$

And the fractional modulation amplitude is therefore simply:

$$\text{Fractional Modulation} = 4|a_0 a_1| \left| \frac{\frac{I_1}{I_0} + \frac{I_1^*}{I_0^*} + \frac{R_1}{R_0} + \frac{R_1^*}{R_0^*}}{a_0^* a_0 + a_1^* a_1} \right|$$

Elements of the theoretical treatment:

1. Calculate the ground state of the SF_6 molecule, in particular the highest occupied molecular orbital (HOMO, in this case the triply degenerate t_1 mode) using standard quantum chemistry packages (GAUSSIAN), also getting the normal mode vibrational frequencies, and the dependence of the polarizability on the normal mode coordinate to first order. Now propagate the vibrational wavefunctions for each Raman-active mode through the first (excitation) pulse, by solving the TDSE numerically:

$$i\frac{\partial}{\partial t}a_{n_i}(t) = \omega(n_i + \frac{1}{2})a_{n_i}(t) - \frac{1}{2}\sum_{A,B} E_A(t)E_B(t)(\alpha_{AB} + \frac{\partial \alpha_{AB}}{\partial Q_i}\sqrt{\frac{1}{2m\omega_i}}\times$$

$$(\sqrt{n_i+1}a_{n_i+1} + \sqrt{n_i}a_{n_i-1}))$$

2. Next calculate the tunneling integral that expresses the rate of electron escape from the HOMO during the ionizing laser pulse:

value of the unperturbed wavefunction at the inner turning point times a declining WKB exponential. If we define the direction of the $\vec{E}$ field as $+\hat{z}$, then in the forbidden region

$$\psi(x,y,z,t) = \psi(x,y,z_{\mathrm{tp1}},t)exp[-\int_{z_{\mathrm{tp1}}}^{z} dz\sqrt{2m(V_{\mathrm{mol}} + V_{\mathrm{laser}} - E)}] \qquad (18)$$

where z_{tp1} is the inner turning point and the path integral is calculated along the z direction parallel to the applied electric field. At the outer turning point, the usual connection

3. Evaluate 3D Semiclassical Gutzwiller/Van-Vleck Propagator during the time between tunneling and recollision:

To model the wavefunction between the times of ionization and recollision, we use the tunneling wavefunction calculated above as a source term for the semiclassical Gutzwiller/ Van Vleck propagator.

$$K(\vec{r}, t; \vec{r}_0, t_0) = (2\pi i)^{-3/2} \sqrt{C(\vec{r}, t; \vec{r}_0, t_0)} \times \exp[iR(\vec{r}, t; \vec{r}_0, t_0) - i\phi] \tag{19}$$

where $R(\vec{r}, t; \vec{r}_0, t_0)$ is the action integral $R = \int L(q, \dot{q}, t)dt$ calculated for the classical trajectory beginning at $(\vec{r}, t)$ and ending at $(\vec{r}_0, t_0)$ and $C(\vec{r}, t; \vec{r}_0, t_0) = |-\frac{\partial^2 R}{\partial \vec{r}_i \partial \vec{r}_j}|$ is the density of trajectories for given initial and final points. ϕ is a phase factor equal to $\frac{\pi}{2}$ times the number of conjugate points crossed by the trajectory. Since electrons reach the continuum by tunnel ionization, we start all trajectories at the classical turning point of the molecular plus laser potential with $\vec{v}_0 = 0$.

The equation for $\psi(\vec{r}_0, t_0)$ in a volume of interest resulting from a surface source term is given by [8]

$$\psi(\vec{r}, t) = \frac{1}{4\pi} \int_0^t dt_0 \int d\vec{S}_0 \cdot [K(\vec{r}, t; \vec{r}_0, t_0) \nabla_0 \psi(\vec{r}_0, t_0) - \psi(\vec{r}_0, t_0) \nabla_0 K(\vec{r}, t, \vec{r}_0, t_0)] \tag{23}$$

where ∇_0 denotes the gradient with respect to $\vec{r}_0$.

Since we consider only trajectories that start with $v_0 = 0$, $\nabla_0 K(\vec{r}, t, \vec{r}_0, t_0) = 0$ and the continuum wavefunction of the electron is given by.

$$\psi_c(\vec{r}, t) = \frac{1}{4\pi} \int_0^t dt_0 \int d\vec{S}_0 \cdot K(\vec{r}, t; \vec{r}_0, t_0) \nabla_0 \psi(\vec{r}_0, t_0)] \tag{24}$$

Setting $v_0 = 0$ has the further property of reducing to just one the number of classical trajectories originating at (r_0, t_0) that must be considered in the Gutzwiller propagator.

4. Join/match the returning wavepacket to ZERO FIELD electron-ion scattering solutions at fixed energies, calculated in a realistic electron-molecule scattering calculation (static exchange level, Stefano Tonzani, finite-element R-matrix method).

tering states will have complicated behavior. Beyond the range of the molecular potential, where the projection is performed, the scattering states are given by:

$$\psi_{E,l;m}(\vec{r}) = \frac{1}{i\sqrt{2}} f_l^-(r) Y_{l,m}(\theta,\phi) - \frac{1}{i\sqrt{2}} f_{l'}^+(r) Y_{l',m'}(\theta,\phi) S_{l,m;l',m'}(E). \tag{25}$$

The scattering wavefunction is then given by

$$\psi_S = \int dE \sum_{l,m} A_{l,m}(E) \psi_{E,l;m} e^{-iEt}, \tag{26}$$

where

$$A_{l,m}(E) = e^{iEt} \int_0^\infty r^2 dr \int d\Omega \psi^*_{E,l;m}(r,\Omega) \psi_c(r,\Omega,t). \tag{27}$$

This projection is simplified using the method of stationary phase. Using equations 20 and 24, $\frac{\partial \psi_c(\vec{r},t)}{\partial \vec{r}} = i\vec{p}\psi_c(\vec{r},t)$.

5. Calculate the coefficients using the method of stationary phase, and then use those coefficients with the zero-field dipole matrix elements for these scattering solutions.

Because the stationary phase condition cancels the first order term in equation 28, the Taylor expansion of the continuum phase, the contribution of a single trajectory and its envelope of closely assosciated trajectories to the projection integral 27 is given by the Gaussian integral [12]

$$A_{l,m}(E) = \int d^3\vec{r} \frac{1}{i\sqrt{2}} f_l^{-*}(r) Y_{l,m}^{*}(\Omega) \psi_c(\vec{r}) exp(\frac{i}{2} \frac{\partial^2 R}{\partial \vec{r}^2} |_{\vec{r}=\vec{r}_f}) \tag{29}$$

which evaluates to

$$A_{l,m}(E) = \frac{1}{i\sqrt{2}} f_l^{-*}(r_f) Y_{l,m}^{*}(\Omega_f) \psi_c(r_f, \Omega_f) (2\pi i)^{3/2} |\frac{\partial^2 R}{\partial \vec{r}_f^2}|^{-1/2} \tag{30}$$

In order to calculate the recombination amplitude, we calculate the recombination amplitude for each scattering state individually in the length gauge. Setting $d_{l,m}(E) = \langle \psi_g | \vec{x} | \psi_{E,l;m} \rangle$, the dipole recombination amplitude is simply $D(E) = \sum_{l,m} A_{l,m}(E) d_{l,m}(E)$.

Repeat this procedure for distorted normal mode coordinates, to get the derivative of the dipole matrix elements w.r.t. Q.

6. Now put it all together to predict the amplitude of modulation of these vibrational quantum beats:

ONE-DIMENSIONAL, TWO-STATE MODEL OF VIBRATIONAL INTERFERENCE

The vibrational wavefunction of a molecule can be expanded as the product of one-dimensional simple harmonic oscillator states of the neutral molecule's various normal modes:

$$|\psi^{\text{vib}}\rangle = \sum_{n_1,n_2,n_3\cdots=0}^{\infty} a_{n_1,n_2,n_3\ldots}\,|n_1, n_2, n_3\ldots\rangle \qquad (1)$$

where n_1, n_2, n_3 are vibrational quantum numbers for the various normal modes.

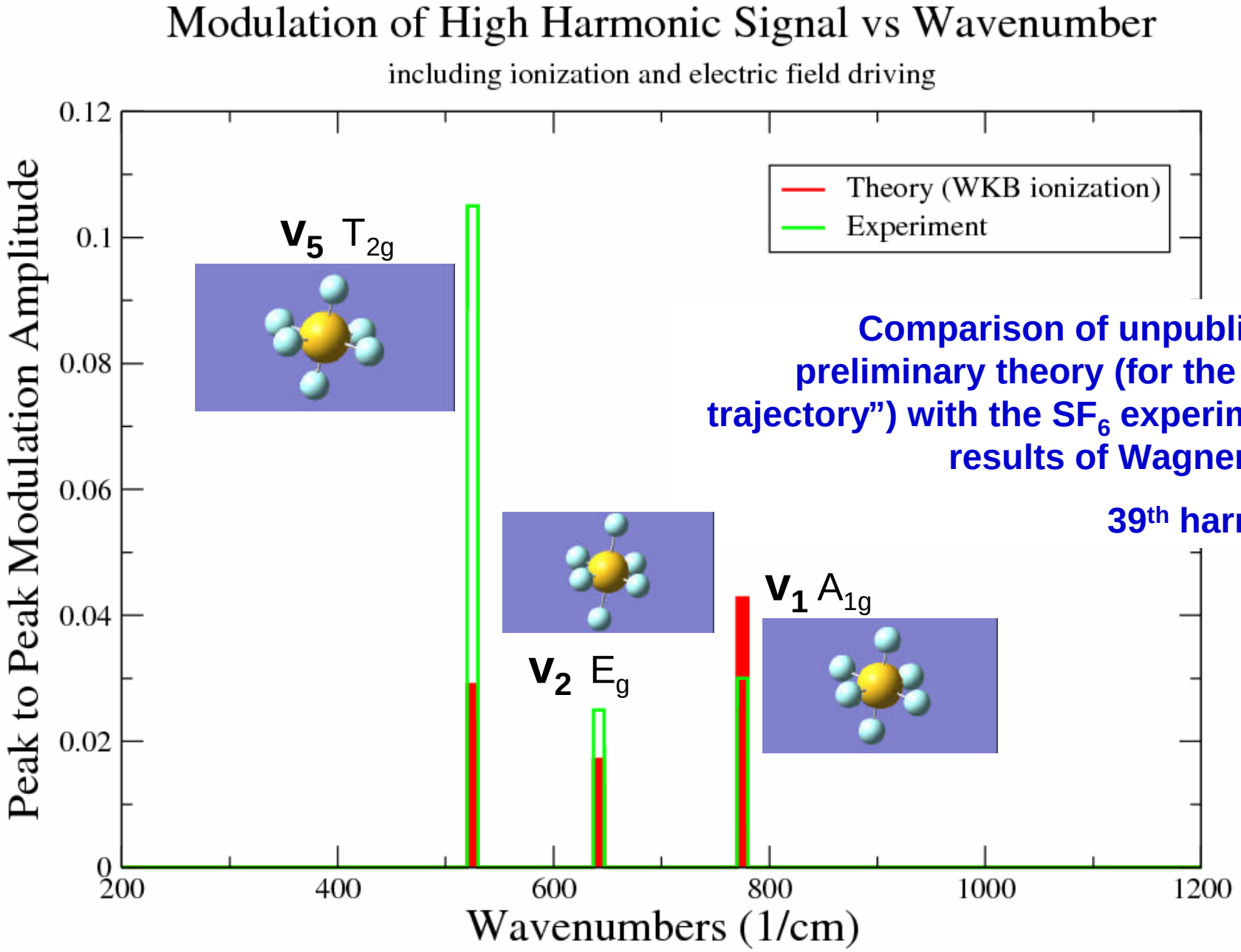

Comparison of unpublished, preliminary theory (for the "long trajectory") with the SF_6 experimental results of Wagner et al.

39^{th} harmonic

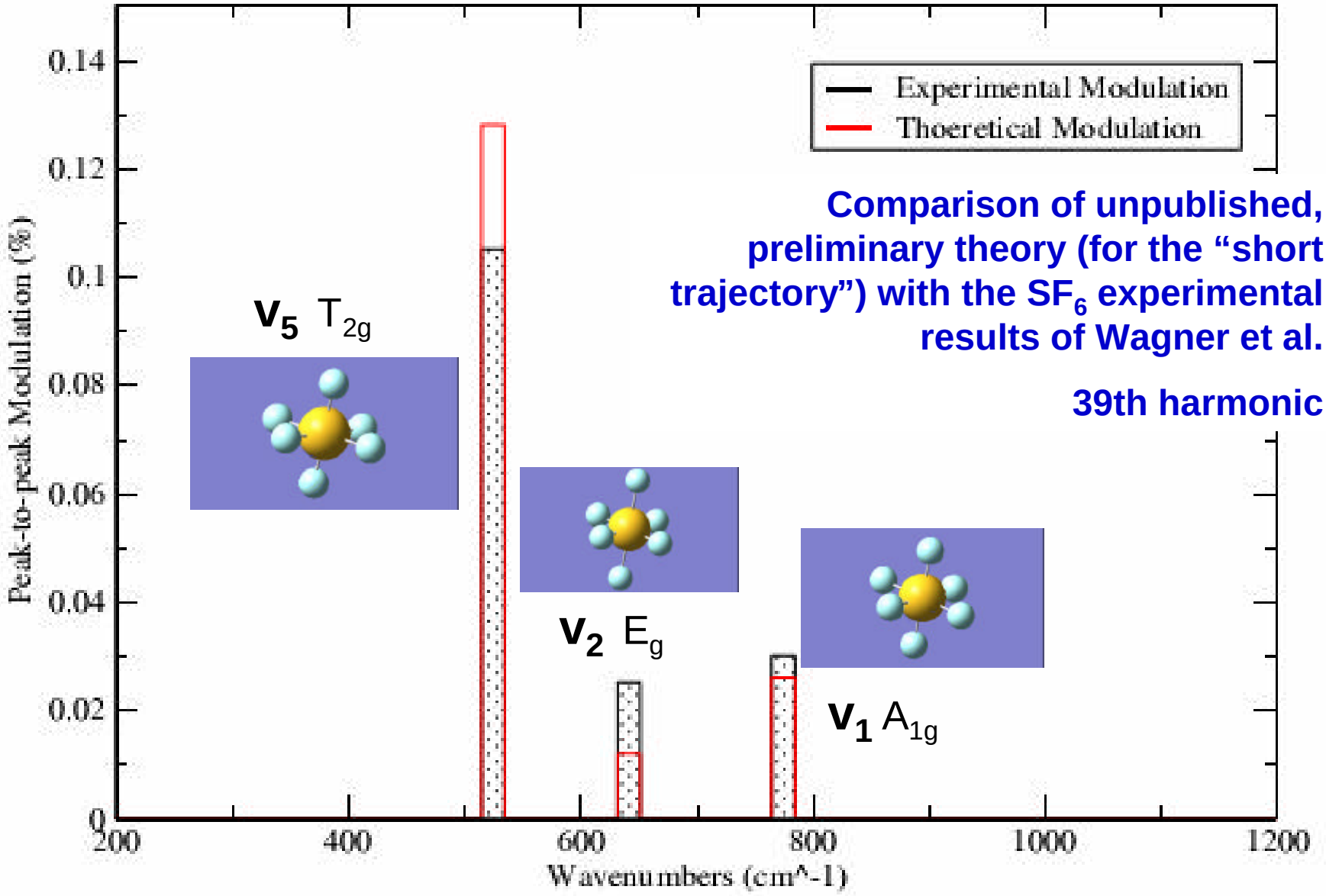

Comparison of unpublished, preliminary theory (for the "short trajectory") with the SF_6 experimental results of Wagner et al.

39th harmonic

Short trajectories, different causes of modulation, t_match*wL=3.8

mode	ionization	recombination	raman	total
A1g	.1447	.1527	2.98E-8	.06196
T2g1	.01469	.02327	8.9E-8	.03757
T2g2	.0264	.0386	2.376E-9	.0639
T2g3	.034	.06417	3.54E-9	.0964
Eg1	.01548	.008048	1.15E-8	.00949
Eg2	.0395	.0146	2.91E-8	.0282

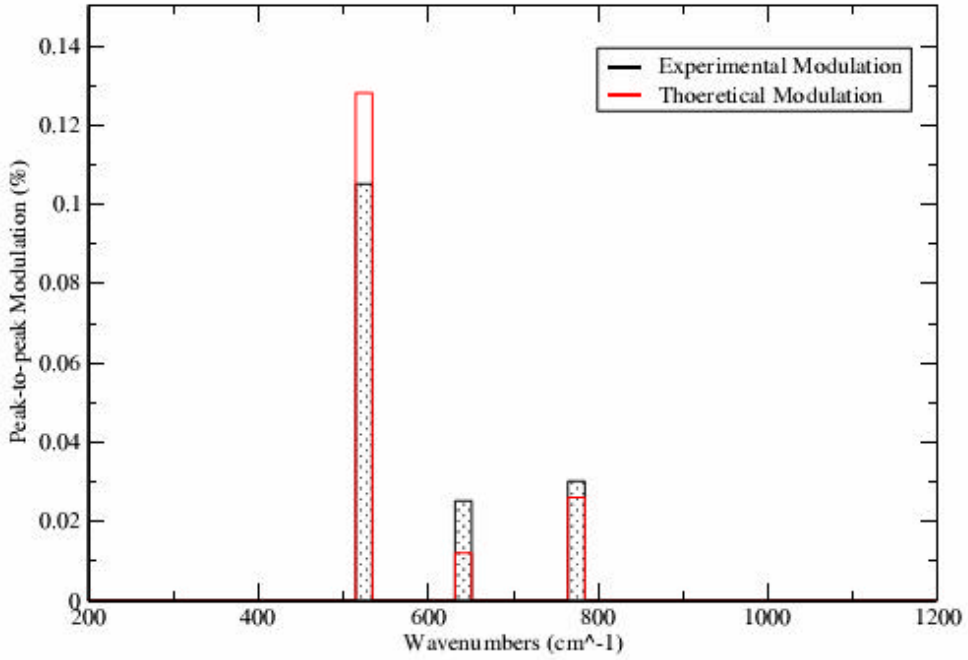

CAUTION: **Preliminary theory!!**

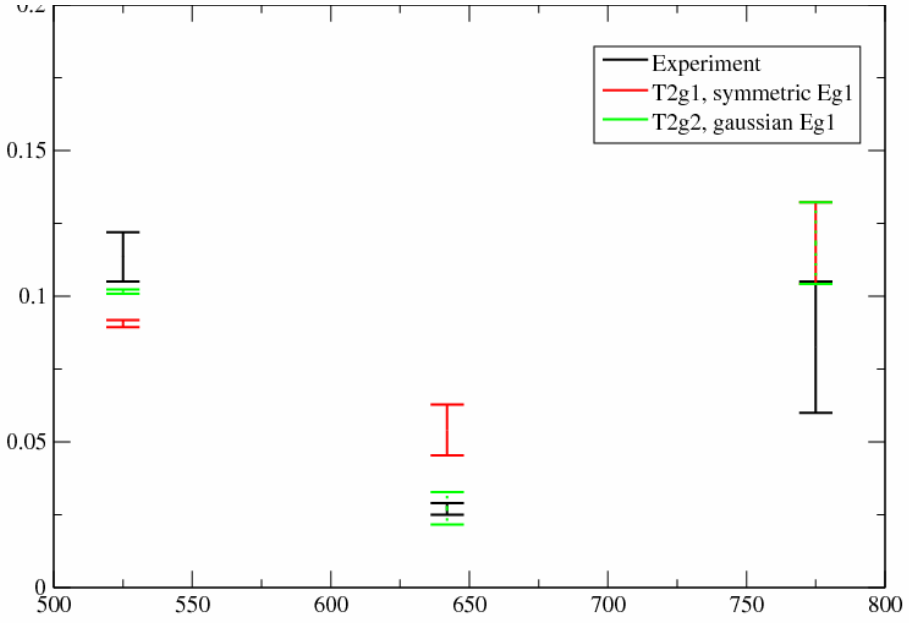

This graph uses integrated experimental peak areas and should be a more reliable representation of the experiment than the *above* figure, which just used the experimental peak height.

The experimental “error bar” shows the range of values obtained in two different runs.

Other interesting physics, not yet incorporated in this model, which might be important:

Jahn-Teller effect on the SF_6^+ ion vibrational dynamics, after the active electron tunnels out